

10th October 2019
BARI-TH/00

The impact of the static part of the Earth's gravity field on some tests of General Relativity with laser-ranging

Lorenzo Iorio[†]

[†]Dipartimento di Fisica dell' Università di Bari, via Amendola 173, 70126, Bari, Italy

Abstract

In this paper we calculate explicitly the secular classical precessions of the node Ω and the perigee ω of an Earth artificial satellite induced by the static, even zonal harmonics of the geopotential up to degree $l = 20$. Subsequently, their systematic errors induced by the mismodelling in the even zonal geopotential coefficients J_l are compared to the general relativistic secular gravitomagnetic and gravitoelectric precessions of the node and the perigee of the existing laser-ranged geodetic satellites and of the proposed LARES. The impact of the future terrestrial gravity models from CHAMP and GRACE missions is discussed as well.

1 Introduction

Recently, great efforts have been devoted to the investigation of the possibility of measuring some tiny general relativistic effects in the gravitational field of the Earth by analyzing the laser-ranged data to some existing or proposed geodetic laser-tracked (SLR) satellites.

The most famous experiment is that performed with LAGEOS and LAGEOS II and aimed to the detection of the gravitomagnetic Lense–Thirring drag of inertial frames [*Lense and Thirring*, 1918; *Ciufolini and Wheeler*, 1995] in the gravitational field of the Earth [*Ciufolini et al.*, 1998]. The analysis of the orbits of the LAGEOS satellites could allow also for the precise measurement of the gravitoelectric perigee advance [*Ciufolini and Wheeler*, 1995] in the gravitational field of the Earth [*Iorio*, 2002; *Iorio et al.*, 2002a]. Moreover, the possibility of including also the data from other existing SLR satellites in these analysis is currently investigated [*Iorio*, 2002]. The proposed LAGEOS III–LARES mission [*Ciufolini*, 1986], whose original configuration is currently being reanalyzed in view of the inclusion of more orbital elements of various SLR satellites in the observable to be adopted, could be of great significance for both gravitomagnetic and gravitoelectric tests [*Iorio et al.*, 2002a; 2002b]. Satellite laser ranging could be the natural candidate also for the implementation of a space-based experiment aimed to the detection of the so called gravitomagnetic clock effect [*Mashhoon et al.*, 1999; *Iorio et al.*, 2002c], which is sensitive to the sense of motion of two counter-orbiting satellites along identical orbits. Finally, the well known ambitious Stanford GP–B experiment [*Everitt et al.*, 2001] is scheduled to fly in fall 2002.

In all such performed or proposed experiments it is of the utmost importance to assess as much reliably as possible the error budget. Indeed, the terrestrial environment is rich of competing classical perturbing forces of gravitational and non-gravitational origin which in many cases are much more larger than the general relativistic effects to be investigated. In particular, it is the impact of the systematic errors induced by the mismodelling in such various classical perturbations which is relevant in determining the total realistic accuracy of an experiment like those previously mentioned.

The gravitomagnetic and gravitoelectric effects of interest here are linear trends affecting the perigee ω and the node Ω of the orbit of a satellite and amounting to 10^1 – 10^3 milliarcseconds per

year (mas/y in the following). Such secular precessions can be measured by means of suitable combinations of the orbital residuals of the rates of the nodes and the perigees of different SLR satellites [Ciufolini, 1996; Iorio, 2002]. Such combinations can be written in the form

$$\sum_{i=1}^N c_i f_i = X_{\text{GR}} \mu_{\text{GR}}, \quad (1)$$

in which the coefficients c_i are suitably built up with the orbital parameters of the satellites entering the combinations, the f_i are the residuals of the rates of the nodes and the perigees of the satellites entering the combination, X_{GR} is the slope, in mas/y, of the general relativistic trend of interest and μ_{GR} is the solve-for parameter, to be determined by means of usual least-square procedures, which accounts for the general relativistic effect. For example, in the case of the Lense–Thirring effect $X_{\text{LT}} = 60.2$ mas/y, while for the gravitoelectric perigee advance $X_{\text{GE}} = 3,348$ mas/y.

In this context the most important source of systematic error is represented by the secular classical precessions of the node and the perigee induced by the mismodelled even ($l = 2n$, $n = 1, 2, 3, \dots$) zonal ($m = 0$) harmonics of the multipolar expansion of the terrestrial gravitational field, called geopotential. Indeed, while the time-varying orbital tidal perturbations [Iorio, 2001; Iorio and Pavlis, 2001; Pavlis and Iorio, 2002] and non-gravitational orbital perturbations [Lucchesi, 2001], according to their periods P and to the adopted observational time span T_{obs} , can be viewed as empirically fitted quantity and can be removed from the signal, this is not the case of the even zonal classical precessions. Their mismodelled linear trends act as superimposed effects which may alias the recovery of the genuine general relativistic features. Such disturbing trends cannot be removed from the signal without canceling also the general relativistic signature, so that one can only assess as more accurately as possible their impact on the measurement. The systematic error induced by the mismodelled part of the geopotential can then be viewed as a sort of unavoidable, lower bound of the total systematic error. Then, the combinations of eq. (1) must be suitably designed in order to reduce as much as possible such error. In particular, the coefficients c_i are calculated in order to cancel out the contributions of the first even zonal mismodelled harmonics which, as we will see later, represent the major source of uncertainty in the Lense–Thirring and gravitoelectric precessions [Ciufolini, 1996; Iorio, 2002].

Table 1: Orbital parameters of the existing spherical passive geodetic laser-ranged satellites and of LARES. Aj=Ajisai, Stl=Stella, Str=Starlette, WS=WESTPAC1, E1=ETALON1, E2=ETALON2, L1=LAGEOS, L2=LAGEOS II, LR=LARES. a is in km, i in deg and n in s^{-1} .

	Aj	Stl	Str	WS	E1	E2	L1	L2	LR
a	7,870	7,193	7,331	7,213	25,498	25,498	12,270	12,163	12,270
e	0.001	0	0.0204	0	0.00061	0.00066	0.0045	0.014	0.04
i	50	98.6	49.8	98	64.9	65.5	110	52.65	70
n	0.0009	0.001	0.001	0.001	0.00015	0.00015	0.00046	0.00047	0.00046

In Tab. 1 we quote the orbital parameters of the existing spherical passive geodetic laser-ranged satellites Ajisai, Stella, Starlette, WESTPAC1, ETALON1, ETALON2, LAGEOS, LAGEOS II and of the proposed LARES. In it a is the semimajor axis, e is the eccentricity, i is the inclination and $n = \sqrt{GMa^{-3}}$, where G is the Newtonian gravitational constant and M is the mass of the central body, is the Keplerian mean motion. It is worth noting that the perigees of many of them, except for Starlette, cannot be employed for any relativistic tests due to the notable smallness of their eccentricities.

In this paper we calculate explicitly, up to $l = 20$, the expressions of the coefficients of the classical secular precessions on the node and the perigee due to the geopotential (section 2). In section 3 we work out the numerical values of these precessions for the existing SLR geodetic satellites and of LARES and compare them to the general relativistic effects. In section 4 we work out the explicit expression of the systematic error affecting the observables of eq. (1). Section 5 is devoted to the conclusions.

2 The orbital classical precessions

Here we show the explicitly calculated coefficients

$$\dot{\Omega}_{.2n} \equiv \frac{\partial \dot{\Omega}_{\text{class}}}{\partial (J_{2n})} \quad (2)$$

and

$$\dot{\omega}_{.2n} \equiv \frac{\partial \dot{\omega}_{\text{class}}}{\partial (J_{2n})} \quad (3)$$

of the satellites' classical nodal and apsidal precessions due to the even zonal harmonics of the geopotential up to $l = 20$. Recall that $J_l \equiv -C_{l0}$, $l = 2n$, $n = 1, 2, 3, \dots$ where the

unnormalized adimensional Stokes coefficients C_{lm} of degree l and order m can be obtained from the normalized \overline{C}_{lm} with

$$C_{lm} = N_{lm} \overline{C}_{lm}. \quad (4)$$

In it

$$N_{lm} = \left[\frac{(2l+1)(2-\delta_{0m})(l-m)!}{(l+m)!} \right]^{\frac{1}{2}}. \quad (5)$$

For the general expression of the classical rates of the near Earth satellites' Keplerian orbital elements due to the geopotential \dot{a}_{class} , \dot{e}_{class} , \dot{i}_{class} , $\dot{\Omega}_{\text{class}}$, $\dot{\omega}_{\text{class}}$, $\dot{\mathcal{M}}_{\text{class}}$, see [Kaula, 1966]. The coefficients $\dot{\Omega}_{.2n}$ and $\dot{\omega}_{.2n}$ are of crucial importance in the evaluation of the systematic error due to the mismodelled even zonal harmonics of the geopotential; moreover, they enter the combined residuals' coefficients c_i of eq. (1). Since the general relativistic effects investigated are secular perturbations, we have considered only the perturbations averaged over one satellite's orbital period. This has been accomplished with the condition $l - 2p + q = 0$. Since the eccentricity functions G_{lpq} are proportional to $e^{|q|}$, for a given value of l we have considered only those values of p which fulfil the condition $l - 2p + q = 0$ with $q = 0$, i.e. $p = \frac{l}{2}$. This implies that in the summations

$$\sum_{p=0}^l \frac{dF_{l0p}}{di} \sum_{q=-\infty}^{+\infty} G_{lpq} \quad (6)$$

and

$$\sum_{p=0}^l F_{l0p} \sum_{q=-\infty}^{+\infty} \frac{dG_{lpq}}{de} \quad (7)$$

involved in the expressions of the classical rates we have considered only $F_{l0\frac{l}{2}}$ and $G_{l\frac{l}{2}0}$. Moreover, in working out the $G_{l\frac{l}{2}0}$ we have neglected the terms of order $\mathcal{O}(e^k)$ with $k > 2$.

2.1 The nodal coefficients

The nodal coefficients, proportional to

$$\frac{1}{\sin i} \sum_{q=-\infty}^{+\infty} G_{lpq} \sum_{p=0}^l \frac{dF_{lmp}}{di}, \quad (8)$$

are (R is the Earth's mean equatorial radius)

$$\dot{\Omega}_{.2} = -\frac{3}{2}n \left(\frac{R}{a} \right)^2 \frac{\cos i}{(1-e^2)^2}, \quad (9)$$

$$\dot{\Omega}_{.4} = \dot{\Omega}_{.2} \left[\frac{5}{8} \left(\frac{R}{a} \right)^2 \frac{(1 + \frac{3}{2}e^2)}{(1 - e^2)^2} (7 \sin^2 i - 4) \right], \quad (10)$$

$$\dot{\Omega}_{.6} = \dot{\Omega}_{.2} \left[\frac{35}{8} \left(\frac{R}{a} \right)^4 \frac{(1 + 5e^2)}{(1 - e^2)^4} \left(\frac{33}{8} \sin^4 i - \frac{9}{2} \sin^2 i + 1 \right) \right], \quad (11)$$

$$\begin{aligned} \dot{\Omega}_{.8} = \dot{\Omega}_{.2} & \left[\frac{105}{16} \left(\frac{R}{a} \right)^6 \frac{(1 + \frac{21}{2}e^2)}{(1 - e^2)^6} \left(\frac{715}{64} \sin^6 i - \frac{143}{8} \sin^4 i + \right. \right. \\ & \left. \left. + \frac{33}{4} \sin^2 i - 1 \right) \right], \end{aligned} \quad (12)$$

$$\begin{aligned} \dot{\Omega}_{.10} = \dot{\Omega}_{.2} & \left[\frac{1,155}{128} \left(\frac{R}{a} \right)^8 \frac{(1 + 18e^2)}{(1 - e^2)^8} \left(\frac{4,199}{128} \sin^8 i - \frac{1,105}{16} \sin^6 i \right. \right. \\ & \left. \left. + \frac{195}{4} \sin^4 i - 13 \sin^2 i + 1 \right) \right], \end{aligned} \quad (13)$$

$$\begin{aligned} \dot{\Omega}_{.12} = \dot{\Omega}_{.2} & \left[\frac{3,003}{256} \left(\frac{R}{a} \right)^{10} \frac{(1 + \frac{55}{2}e^2)}{(1 - e^2)^{10}} \left(\frac{52,003}{512} \sin^{10} i - \frac{33,915}{128} \sin^8 i \right. \right. \\ & \left. \left. + \frac{8,075}{32} \sin^6 i - \frac{425}{4} \sin^4 i + \frac{75}{4} \sin^2 i - 1 \right) \right], \end{aligned} \quad (14)$$

$$\begin{aligned} \dot{\Omega}_{.14} = \dot{\Omega}_{.2} & \left[\frac{15,015}{1,024} \left(\frac{R}{a} \right)^{12} \frac{(1 + \frac{91}{2}e^2)}{(1 - e^2)^{12}} \left(\frac{334,305}{1,024} \sin^{12} i - \frac{260,015}{256} \sin^{10} i \right. \right. \\ & \left. \left. + \frac{156,009}{128} \sin^8 i - \frac{11,305}{16} \sin^6 i + \frac{1,615}{8} \sin^4 i - \frac{51}{2} \sin^2 i + 1 \right) \right], \end{aligned} \quad (15)$$

$$\begin{aligned} \dot{\Omega}_{.16} = \dot{\Omega}_{.2} & \left[\frac{36,465}{2,048} \left(\frac{R}{a} \right)^{14} \frac{(1 + \frac{105}{2}e^2)}{(1 - e^2)^{14}} \left(\frac{17,678,835}{16,384} \sin^{14} i - \right. \right. \\ & - \frac{3,991,995}{1,024} \sin^{12} i + \frac{2,890,755}{512} \sin^{10} i - \frac{535,325}{128} \sin^8 i + \frac{107,065}{64} \sin^6 i \\ & \left. \left. - \frac{2,793}{8} \sin^4 i + \frac{133}{4} \sin^2 i - 1 \right) \right], \end{aligned} \quad (16)$$

$$\begin{aligned} \dot{\Omega}_{.18} = \dot{\Omega}_{.2} & \left[\frac{692,835}{32,768} \left(\frac{R}{a} \right)^{16} \frac{(1 + 68e^2)}{(1 - e^2)^{16}} \left(\frac{119,409,675}{32,768} \sin^{16} i - \right. \right. \\ & - \frac{30,705,345}{2,048} \sin^{14} i + \frac{6,513,255}{256} \sin^{12} i - \frac{1,470,735}{64} \sin^{10} i + \\ & \left. \left. + \frac{760,725}{64} \sin^8 i - \frac{28,175}{8} \sin^6 i + \right. \right. \end{aligned}$$

$$+ \frac{1,127}{2} \sin^4 i - 42 \sin^2 i + 1) \Big], \quad (17)$$

$$\begin{aligned} \dot{\Omega}_{.20} = & \dot{\Omega}_{.2} \left[\frac{1,616,615}{65,536} \left(\frac{R}{a} \right)^{18} \frac{(1 + \frac{171}{2}e^2)}{(1 - e^2)^{18}} \left(\frac{1,641,030,105}{131,072} \sin^{18} i \right. \right. \\ & - \frac{1,893,496,275}{32,768} \sin^{16} i + \frac{460,580,175}{4,096} \sin^{14} i - \frac{30,705,345}{256} \sin^{12} i \\ & + \frac{19,539,765}{256} \sin^{10} i - \frac{1,890,945}{64} \sin^8 i + \frac{108,675}{16} \sin^6 i - \\ & \left. \left. - \frac{1,725}{2} \sin^4 i + \frac{207}{4} \sin^2 i - 1 \right) \right]. \quad (18) \end{aligned}$$

2.2 The perigee coefficients

The coefficients of the classical perigee precession are much more involved because they are proportional to

$$- \left(\frac{\cos i}{\sin i} \right) \sum_{q=-\infty}^{+\infty} G_{lpq} \sum_{p=0}^l \frac{dF_{lmp}}{di} + \frac{(1 - e^2)}{e} \sum_{q=-\infty}^{+\infty} \frac{dG_{lpq}}{de} \sum_{p=0}^l F_{lmp}. \quad (19)$$

We can pose $\dot{\omega}_{.2n} = \dot{\omega}_{.2n}^a + \dot{\omega}_{.2n}^b$.

The first set is given by (R is the Earth's mean equatorial radius)

$$\dot{\omega}_{.2}^a = \frac{3}{2}n \left(\frac{R}{a} \right)^2 \frac{\cos^2 i}{(1 - e^2)^2}, \quad (20)$$

$$\dot{\omega}_{.4}^a = \dot{\omega}_{.2}^a \left[\frac{5}{8} \left(\frac{R}{a} \right)^2 \frac{(1 + \frac{3}{2}e^2)}{(1 - e^2)^2} (7 \sin^2 i - 4) \right], \quad (21)$$

$$\dot{\omega}_{.6}^a = \dot{\omega}_{.2}^a \left[\frac{35}{8} \left(\frac{R}{a} \right)^4 \frac{(1 + 5e^2)}{(1 - e^2)^4} \left(\frac{33}{8} \sin^4 i - \frac{9}{2} \sin^2 i + 1 \right) \right], \quad (22)$$

$$\begin{aligned} \dot{\omega}_{.8}^a = & \dot{\omega}_{.2}^a \left[\frac{105}{16} \left(\frac{R}{a} \right)^6 \frac{(1 + \frac{21}{2}e^2)}{(1 - e^2)^6} \left(\frac{715}{64} \sin^6 i - \right. \right. \\ & \left. \left. - \frac{143}{8} \sin^4 i + \frac{33}{4} \sin^2 i - 1 \right) \right], \quad (23) \end{aligned}$$

$$\dot{\omega}_{.10}^a = \dot{\omega}_{.2}^a \left[\frac{1,155}{128} \left(\frac{R}{a} \right)^8 \frac{(1 + 18e^2)}{(1 - e^2)^8} \left(\frac{4,199}{128} \sin^8 i - \frac{1,105}{16} \sin^6 i \right. \right.$$

$$+ \frac{195}{4} \sin^4 i - 13 \sin^2 i + 1) \Big], \quad (24)$$

$$\begin{aligned} \dot{\omega}_{.12}^a &= \dot{\omega}_{.2}^a \left[\frac{3,003}{256} \left(\frac{R}{a} \right)^{10} \frac{(1 + \frac{55}{2}e^2)}{(1 - e^2)^{10}} \left(\frac{52,003}{512} \sin^{10} i - \frac{33,915}{128} \sin^8 i \right. \right. \\ &\quad \left. \left. + \frac{8,075}{32} \sin^6 i - \frac{425}{4} \sin^4 i + \frac{75}{4} \sin^2 i - 1 \right) \right], \quad (25) \end{aligned}$$

$$\begin{aligned} \dot{\omega}_{.14}^a &= \dot{\omega}_{.2}^a \left[\frac{15,015}{1,024} \left(\frac{R}{a} \right)^{12} \frac{(1 + \frac{91}{2}e^2)}{(1 - e^2)^{12}} \left(\frac{334,305}{1,024} \sin^{12} i - \frac{260,015}{256} \sin^{10} i + \right. \right. \\ &\quad \left. \left. + \frac{156,009}{128} \sin^8 i - \frac{11,305}{16} \sin^6 i + \frac{1,615}{8} \sin^4 i - \right. \right. \\ &\quad \left. \left. - \frac{51}{2} \sin^2 i + 1 \right) \right], \quad (26) \end{aligned}$$

$$\begin{aligned} \dot{\omega}_{.16}^a &= \dot{\omega}_{.2}^a \left[\frac{36,465}{2,048} \left(\frac{R}{a} \right)^{14} \frac{(1 + \frac{105}{2}e^2)}{(1 - e^2)^{14}} \left(\frac{17,678,835}{16,384} \sin^{14} i - \frac{3,991,995}{1,024} \sin^{12} i \right. \right. \\ &\quad \left. \left. + \frac{2,890,755}{512} \sin^{10} i - \frac{535,325}{128} \sin^8 i + \frac{107,065}{64} \sin^6 i \right. \right. \\ &\quad \left. \left. - \frac{2,793}{8} \sin^4 i + \frac{133}{4} \sin^2 i - 1 \right) \right], \quad (27) \end{aligned}$$

$$\begin{aligned} \dot{\omega}_{.18}^a &= \dot{\omega}_{.2}^a \left[\frac{692,835}{32,768} \left(\frac{R}{a} \right)^{16} \frac{(1 + 68e^2)}{(1 - e^2)^{16}} \left(\frac{119,409,675}{32,768} \sin^{16} i - \right. \right. \\ &\quad \left. \left. - \frac{30,705,345}{2,048} \sin^{14} i + \frac{6,513,255}{256} \sin^{12} i - \frac{1,470,735}{64} \sin^{10} i + \right. \right. \\ &\quad \left. \left. + \frac{760,725}{64} \sin^8 i - \frac{28,175}{8} \sin^6 i + \frac{1,127}{2} \sin^4 i - \right. \right. \\ &\quad \left. \left. - 42 \sin^2 i + 1 \right) \right], \quad (28) \end{aligned}$$

$$\dot{\omega}_{.20}^a = \dot{\omega}_{.2}^a \left[\frac{1,616,615}{65,536} \left(\frac{R}{a} \right)^{18} \frac{(1 + \frac{171}{2}e^2)}{(1 - e^2)^{18}} \left(\frac{1,641,030,105}{131,072} \sin^{18} i \right. \right.$$

$$\begin{aligned}
& - \frac{1,893,496,275}{32,768} \sin^{16} i + \frac{460,580,175}{4,096} \sin^{14} i - \frac{30,705,345}{256} \sin^{12} i \\
& + \frac{19,539,765}{256} \sin^{10} i - \frac{1,890,945}{64} \sin^8 i + \frac{108,675}{16} \sin^6 i - \\
& - \left[\frac{1,725}{2} \sin^4 i + \frac{207}{4} \sin^2 i - 1 \right]. \tag{29}
\end{aligned}$$

The second set is given by (R is the Earth's mean equatorial radius)

$$w_{.2} = -\frac{3}{2}n \left(\frac{R}{a}\right)^2, \tag{30}$$

$$\dot{\omega}_{.2}^b = w_{.2} \left\{ \left[\frac{1}{(1-e^2)^2} \right] \left(\frac{3}{2} \sin^2 i - 1 \right) \right\}, \tag{31}$$

$$\begin{aligned}
\dot{\omega}_{.4}^b &= w_{.2} \left\{ \frac{5}{8} \left(\frac{R}{a}\right)^2 \left[\frac{3}{(1-e^2)^3} + 7 \frac{(1+\frac{3}{2}e^2)}{(1-e^2)^4} \right] \left(\frac{7}{4} \sin^4 i - \right. \right. \\
& \left. \left. - 2 \sin^2 i + \frac{2}{5} \right) \right\}, \tag{32}
\end{aligned}$$

$$\begin{aligned}
\dot{\omega}_{.6}^b &= w_{.2} \left\{ \frac{35}{8} \left(\frac{R}{a}\right)^4 \left[\frac{10}{(1-e^2)^5} + 11 \frac{(1+5e^2)}{(1-e^2)^6} \right] \left(\frac{33}{48} \sin^6 i \right. \right. \\
& \left. \left. - \frac{9}{8} \sin^4 i + \frac{1}{2} \sin^2 i - \frac{1}{21} \right) \right\}, \tag{33}
\end{aligned}$$

$$\begin{aligned}
\dot{\omega}_{.8}^b &= w_{.2} \left\{ \frac{105}{16} \left(\frac{R}{a}\right)^6 \left[\frac{21}{(1-e^2)^7} + 15 \frac{(1+\frac{21}{2}e^2)}{(1-e^2)^8} \right] \left(\frac{715}{512} \sin^8 i \right. \right. \\
& \left. \left. - \frac{143}{48} \sin^6 i + \frac{33}{16} \sin^4 i - \frac{1}{2} \sin^2 i + \frac{1}{36} \right) \right\}, \tag{34}
\end{aligned}$$

$$\begin{aligned}
\dot{\omega}_{.10}^b &= w_{.2} \left\{ \frac{1,155}{128} \left(\frac{R}{a}\right)^8 \left[\frac{36}{(1-e^2)^9} + 19 \frac{(1+18e^2)}{(1-e^2)^{10}} \right] \left(\frac{4,199}{1,280} \sin^{10} i \right. \right. \\
& \left. \left. - \frac{1,105}{128} \sin^8 i + \frac{195}{24} \sin^6 i - \frac{13}{4} \sin^4 i + \frac{1}{2} \sin^2 i - \frac{1}{55} \right) \right\}, \tag{35}
\end{aligned}$$

$$\begin{aligned}
\dot{\omega}_{.12}^b &= w_{.2} \left\{ \frac{3,003}{256} \left(\frac{R}{a}\right)^{10} \left[\frac{55}{(1-e^2)^{11}} + 23 \frac{(1+\frac{55}{2}e^2)}{(1-e^2)^{12}} \right] \left(\frac{52,003}{6,144} \sin^{12} i \right. \right. \\
& \left. \left. - \frac{6,783}{256} \sin^{10} i + \frac{8,075}{256} \sin^8 i - \frac{425}{24} \sin^6 i + \frac{75}{16} \sin^4 i \right. \right.
\end{aligned}$$

$$- \frac{1}{2} \sin^2 i + \frac{1}{78} \Big) \Big\} , \quad (36)$$

$$\begin{aligned} \dot{\omega}_{.14}^b &= w_{.2} \left\{ \frac{15,015}{1,024} \left(\frac{R}{a} \right)^{12} \left[\frac{91}{(1-e^2)^{13}} + 27 \frac{(1 + \frac{91}{2} e^2)}{(1-e^2)^{14}} \right] \times \right. \\ &\times \left(\frac{334,305}{14,336} \sin^{14} i - \frac{260,015}{3,072} \sin^{12} i + \frac{156,009}{1,280} \sin^{10} i - \right. \\ &\left. \left. - \frac{11,305}{128} \sin^8 i + \frac{1,615}{48} \sin^6 i - \frac{51}{8} \sin^4 i + \right. \right. \end{aligned}$$

$$\left. \left. + \frac{1}{2} \sin^2 i - \frac{1}{105} \right) \right\} , \quad (37)$$

$$\begin{aligned} \dot{\omega}_{.16}^b &= w_{.2} \left\{ \frac{36,465}{2,048} \left(\frac{R}{a} \right)^{14} \left[\frac{105}{(1-e^2)^{15}} + 31 \frac{(1 + \frac{105}{2} e^2)}{(1-e^2)^{16}} \right] \times \right. \\ &\times \left(\frac{17,678,835}{262,144} \sin^{16} i - \frac{570,285}{2,048} \sin^{14} i + \frac{963,585}{2,048} \sin^{12} i - \right. \\ &\left. \left. - \frac{107,065}{256} \sin^{10} i + \frac{107,065}{512} \sin^8 i - \frac{931}{16} \sin^6 i + \right. \right. \end{aligned}$$

$$\left. \left. + \frac{133}{16} \sin^4 i - \frac{1}{2} \sin^2 i + \frac{1}{136} \right) \right\} , \quad (38)$$

$$\begin{aligned} \dot{\omega}_{.18}^b &= w_{.2} \left\{ \frac{692,835}{32,768} \left(\frac{R}{a} \right)^{16} \left[\frac{136}{(1-e^2)^{17}} + 35 \frac{(1 + 68e^2)}{(1-e^2)^{18}} \right] \times \right. \\ &\times \left(\frac{39,803,225}{196,608} \sin^{18} i - \frac{30,705,345}{32,768} \sin^{16} i + \frac{930,465}{512} \sin^{14} i - \right. \\ &\left. \left. - \frac{490,245}{256} \sin^{12} i + \frac{152,145}{128} \sin^{10} i - \frac{28,175}{64} \sin^8 i + \right. \right. \end{aligned}$$

$$\left. \left. + \frac{1,127}{12} \sin^6 i - \frac{21}{2} \sin^4 i + \frac{1}{2} \sin^2 i - \frac{1}{171} \right) \right\} , \quad (39)$$

$$\dot{\omega}_{.20}^b = w_{.2} \left\{ \frac{1,616,615}{65,536} \left(\frac{R}{a} \right)^{18} \left[\frac{171}{(1-e^2)^{19}} + 39 \frac{(1 + \frac{171}{2} e^2)}{(1-e^2)^{20}} \right] \times \right.$$

$$\begin{aligned}
& \times \left(\frac{328,206,021}{524,288} \sin^{20} i - \frac{210,388,475}{65,536} \sin^{18} i + \frac{460,580,175}{65,536} \sin^{16} i - \right. \\
& - \frac{30,705,345}{3,584} \sin^{14} i + \frac{6,513,255}{1,024} \sin^{12} i - \frac{378,189}{128} \sin^{10} i + \\
& + \frac{108,675}{128} \sin^8 i - \frac{575}{4} \sin^6 i + \frac{207}{16} \sin^4 i - \\
& \left. - \frac{1}{2} \sin^2 i + \frac{1}{210} \right) \}. \tag{40}
\end{aligned}$$

3 The mismodelled classical precessions

The results obtained in the previous section can be used in working out explicitly the contributions of the mismodelled classical nodal and apsidal precessions up to degree $l = 20$ of the existing spherical passive laser-ranged geodetic satellites and of the proposed LARES. They are of the form $\delta \dot{\Omega}_{(2n)} = \dot{\Omega}_{.2n} \times \delta J_{2n}$, $n = 1, 2, \dots, 10$ and $\delta \dot{\omega}_{(2n)} = \dot{\omega}_{.2n} \times \delta J_{2n}$, $n = 1, 2, \dots, 10$. The coefficients $\dot{\Omega}_{.2n}$ and $\dot{\omega}_{.2n}$ are worked out in section 2 and the values employed for $\delta J_{2n} = \sqrt{4n+1} \times \delta \bar{C}_{2n 0}$, $n = 1, 2, \dots, 10$ are those quoted in EGM96 model [Lemoine *et al.*, 1998].

From Tab. 2 it is interesting to note that for the satellites orbiting at lower altitudes than the LAGEOS satellites the impact of the mismodelled part of the geopotential does not reduce to the first two or three even zonal harmonics. It is confirmed by Fig. 1 and Fig. 2. This feature is very important in calculating the error budget, especially if some combinations including the nodes of low-orbiting satellites are to be considered. Moreover, while for the LAGEOS family a calculation up to $l = 20$ is rather adequate, this is not the case for the other satellites for which the even zonal harmonics of degree $l > 20$ should be considered as well. In regard to this topic, the choice of the Earth gravity model becomes crucial because EGM96, for example, would be not particularly reliable at degrees higher than 20. The same considerations hold also for the perigee whose mismodelled classical precessions are quoted in Tab. 3. We have considered only LAGEOS II, Starlette and the LARES due to the extreme smallness of the eccentricity of the other satellites. Both from Tab. 2 and Tab. 3 the need of cancelling out the first two or three even zonal harmonics from the observable to be adopted, at least for those involving the

Table 2: Mismodelled classical nodal precessions $\delta\dot{\Omega}_{(2n)}$ and predicted Lense-Thirring nodal precessions $\dot{\Omega}_{LT}$ of the existing geodetic laser-ranged satellites and of LARES. L1=LAGEOS, L2=LAGEOS II, LR=LARES, Aj=Ajisai, Stl=Stella, Str=Starlette, WS=WESTPAC1, E1=ETALON1, E2=ETALON2. All the values are in mas/y. For the ETALON satellites, when the values are less than 10^{-4} mas/y a – has been inserted.

$2n$	L1	L2	LR	Aj	Stl	Str	WS	E1	E2
2	-33.4	61	33.4	296.8	-94.6	382.3	-87.1	3.2	3.1
4	-48.3	17.4	48.7	51.5	-519	59.5	-479.2	0.8	0.8
6	-17	-26.1	17.3	-809.7	-912.2	-1,397.7	-847.9	0.03	0.03
8	-1.9	-10.3	2	-366.3	-1,487.2	-674.4	-1,399.7	-0.005	-0.004
10	2.1	3.1	-2.2	823.5	-1,855	1,933.4	-1,781.8	-0.001	–
12	1.6	2.5	-1.7	647.5	-2,144.6	1,636.4	-2,126.6	–	–
14	0.6	-0.007	-0.6	-542.6	-1,963.4	-1,780.9	-2,049.4	–	–
16	0.09	-0.2	-0.1	-517.2	-1,204.6	-1,787.9	-1,376.8	–	–
18	-0.007	-0.03	0.008	117.9	-512.4	580	-717	–	–
20	-0.01	0.01	0.01	247.6	-79.5	1,177	-309	–	–
$\dot{\Omega}_{LT}$	30.7	31.6	30.8	116.7	152.8	144.4	151.5	3.4	3.4

LAGEOS satellites, become quite apparent.

4 The systematic zonal error

Here we expose how to calculate the systematic error due to the mismodelled even zonal harmonics of the geopotential for the combinations involving the residuals of the nodes and the perigees of various satellites.

In general, if we have an observable q which is a function $q = q(x_j)$, $j = 1, 2 \dots M$ of M correlated parameters x_j the error in it is given by

$$\delta q = \left[\sum_{j=1}^M \left(\frac{\partial q}{\partial x_j} \right)^2 \sigma_j^2 + 2 \sum_{h \neq k=1}^M \left(\frac{\partial q}{\partial x_h} \right) \left(\frac{\partial q}{\partial x_k} \right) \sigma_{hk}^2 \right]^{\frac{1}{2}} \quad (41)$$

in which $\sigma_j^2 \equiv C_{jj}$ and $\sigma_{hk}^2 \equiv C_{hk}$ where $\{C_{hk}\}$ is the square matrix of covariance of the parameters x_j .

In our case the observable q is any residuals' combination

$$q = \sum_{i=1}^N c_i f_i(x_j), \quad j = 1, 2 \dots 10, \quad (42)$$

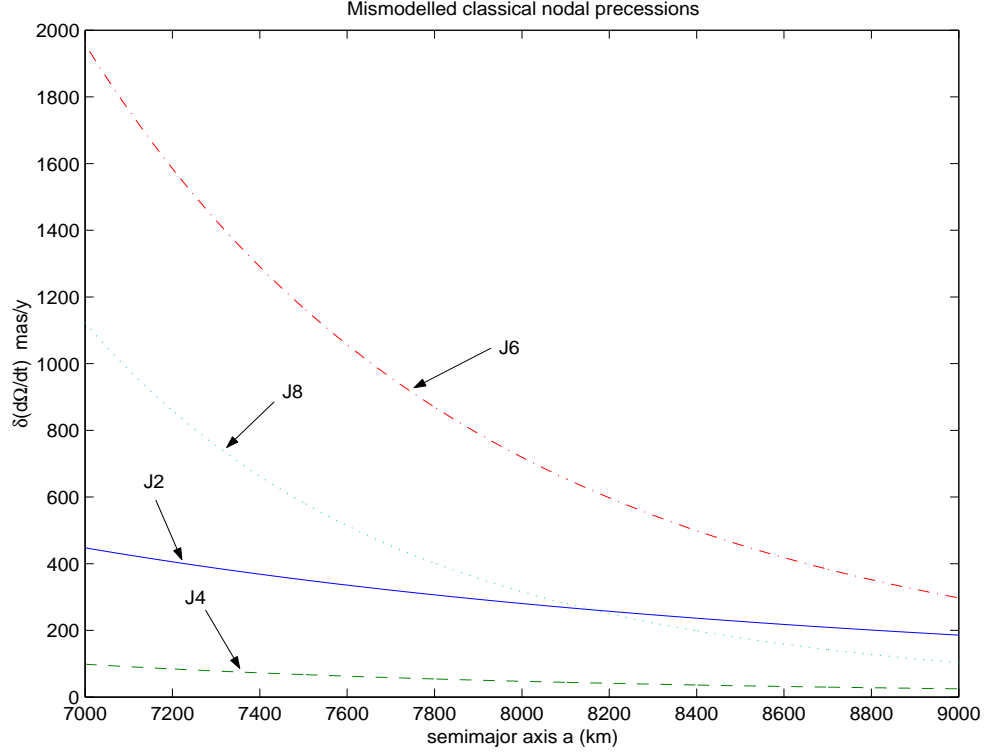


Figure 1: Mismodelled classical nodal precessions $\delta\dot{\Omega}_{(2n)}$ for a typical orbital configuration with $i = 50$ deg, $e = 0.02$. The semimajor axis spans from 7,000 km to 9,000 km. The harmonics considered are J_2 , J_4 , J_6 , J_8 . The errors in them are those released in EGM96 gravity model.

where x_j , $j = 1, 2, \dots, 10$ are the even zonal geopotential's coefficients J_2, J_4, \dots, J_{20} , the f_i , $i = 1, 2, \dots, N$ are the residuals of the precessions of the nodes $\delta\dot{\Omega}$ and the perigees $\delta\dot{\omega}$ of the satellites employed, the c_i , $i = 1, 2, \dots, N$ are the coefficients of the residuals entering the combinations, and N is the number of orbital nodal or apsidal residuals entering the combination. Recall that the coefficients c_i may be either constant or depend on the orbital elements of the satellites entering the combinations through the coefficients $\dot{\Omega}_{.2n}$ and $\dot{\omega}_{.2n}$ worked out in section 2. Since

$$\frac{\partial q}{\partial x_j} = \sum_{i=1}^N c_i \frac{\partial f_i}{\partial x_j}, \quad j = 1, 2, \dots, 10, \quad (43)$$

by putting eq. (43) in eq. (41) one obtains, in mas/y

$$\delta q = \left[\sum_{j=1}^{10} \left(\sum_{i=1}^N c_i \frac{\partial f_i}{\partial x_j} \right)^2 \sigma_j^2 + 2 \sum_{h \neq k=1}^{10} \left(\sum_{i=1}^N c_i \frac{\partial f_i}{\partial x_h} \right) \left(\sum_{i=1}^N c_i \frac{\partial f_i}{\partial x_k} \right) \sigma_{hk}^2 \right]^{\frac{1}{2}}. \quad (44)$$

The covariance matrix is that of EGM96 gravity model [Lemoine *et al.*, 1998]. The percent error, for a given general relativistic trend and for a given combination, is obtained by taking

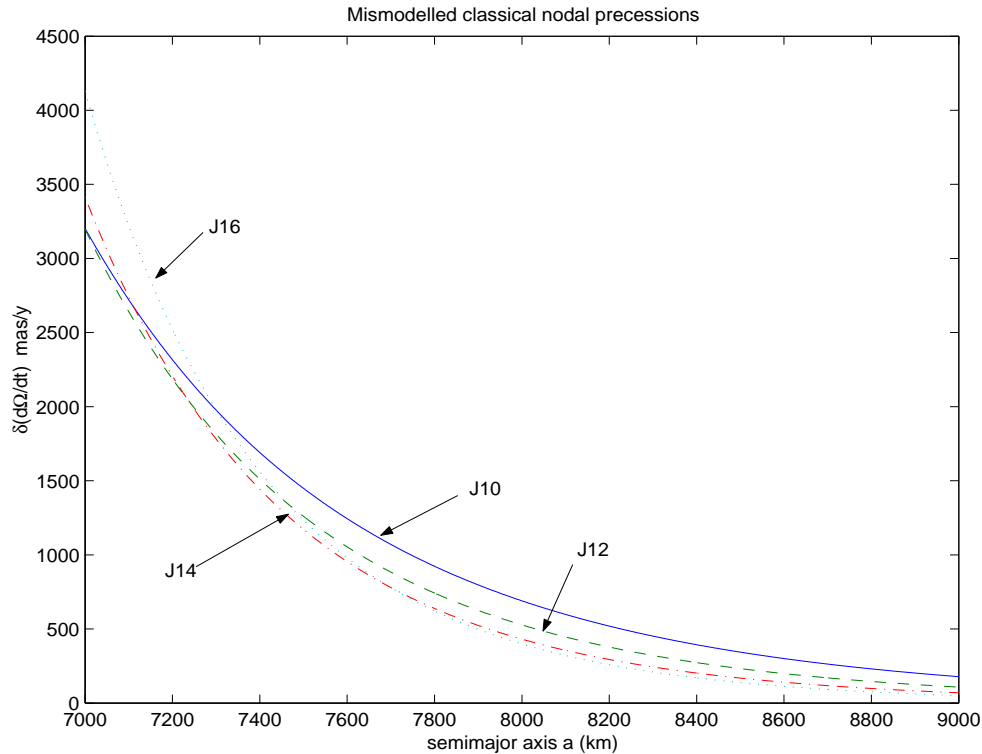


Figure 2: Mismodelled classical nodal precessions $\delta\dot{\Omega}_{(2n)}$ for a typical orbital configuration with $i = 50$ deg, $e = 0.02$. The semimajor axis spans from 7,000 km to 9,000 km. The harmonics considered are J_{10} , J_{12} , J_{14} , J_{16} . The errors in them are those released in EGM96 gravity model.

the ratio of eq. (44) to the slope in mas/y of the general relativistic trend for the residual combination considered.

The validity of eq. (44) has been checked by calculating with it the systematic error due to the even zonal harmonics of the geopotential of the gravitomagnetic LAGEOS experiment; indeed the result

$$\delta\mu_{LT} = 12.9\% \mu_{LT} \quad (45)$$

claimed in [Ciufolini et al., 1998] has been obtained again. For the systematic error due to the even zonal harmonics of the geopotential of alternative proposed gravitomagnetic and gravito-electric experiments, see [Iorio, 2002; Iorio et al., 2002a].

A very important point to stress is that the forthcoming new data on the Earth's gravitational field by CHAMP, which has been launched in July 2000, and GRACE, which has been launched in March 2002, will have a great impact on the reduction of the systematic error due

Table 3: Mismodelled classical perigee precessions $\delta\dot{\omega}_{(2n)}$ and predicted Lense-Thirring and gravitoelectric perigee precessions $\dot{\omega}_{\text{LT}}$ and $\dot{\omega}_{\text{GE}}$ of the existing spherical passive geodetic laser-ranged satellites and of LARES. L1=LAGEOS, L2=LAGEOS II, LR=LARES, Aj=Ajisai, Stl=Stella, Str=Starlette, WS=WESTPAC1, E1=ETALON1, E2=ETALON2. All the values are in mas/y.

$2n$	L1	L2	LR	Aj	Stl	Str	WS	E1	E2
2	–	-42.3	20.3	–	–	-320.7	–	–	–
4	–	-122.7	-17.6	–	–	-1,924.4	–	–	–
6	–	-18.2	-49.2	–	–	429.1	–	–	–
8	–	43.1	-42.6	–	–	6,355.8	–	–	–
10	–	19.5	-18	–	–	2,805.1	–	–	–
12	–	-5.3	-3	–	–	-10,862.2	–	–	–
14	–	-6.2	2	–	–	-10,774.7	–	–	–
16	–	-0.2	1.3	–	–	8,395.8	–	–	–
18	–	0.4	0.4	–	–	9,086.4	–	–	–
20	–	0.1	0.08	–	–	-3,043.3	–	–	–
$\dot{\omega}_{\text{LT}}$	–	-57.5	-31.6	–	–	68.5	–	–	–
$\dot{\omega}_{\text{GE}}$	–	3,348	3,278.6	–	–	11,804.7	–	–	–

to the mismodelled part of geopotential. Indeed, they will yield, among other things, more accurately determined geopotential coefficients J_{2n} , especially those of high degrees whose relative accuracy is lower than that of the low degrees coefficients.

In order to get a preliminary insight of what the improvement due to the new Earth gravity models might be, in Tab. 4 and Tab. 5 we present the mismodelled nodal and apsidal classical precessions according to the very preliminary satellite-only solution EIGEN-1S obtained including 88 days of data from CHAMP available at <http://op.gfz-potsdam.de/champ/results/grav/>. Let us consider, for example, the usual observable by Ciufolini [Ciufolini, 1996] for the detection of the Lense-Thirring drag

$$\delta\dot{\Omega}^{\text{I}} + 0.295 \times \delta\dot{\Omega}^{\text{II}} - 0.35 \times \delta\dot{\omega}^{\text{II}} \sim 60.2\mu_{\text{LT}}. \quad (46)$$

The root-sum-square error due to geopotential, according to the diagonal part only of the covariance matrix of EGM96 model, amounts to 46.5% (it reduces to 12.9% by considering also the correlation among the spherical harmonics coefficients); according to the diagonal part only of the covariance matrix of EIGEN-1S (at present, its full covariance matrix is not yet publicly available), it reduces to 10.5%.

If we consider the combination proposed in [Iorio, 2002]

$$\delta\dot{\Omega}^{\text{I}} + 0.444 \times \delta\dot{\Omega}^{\text{II}} - 0.027 \times \delta\dot{\Omega}^{\text{Aji}} - 0.341 \times \delta\dot{\omega}^{\text{II}} \sim 61.2\mu_{\text{LT}}, \quad (47)$$

in this case the root-sum-square error due to geopotential, according to the diagonal part only of the covariance matrix of EGM96 model, amounts to 64.2% (it reduces to 10.8% by considering also the correlation among the spherical harmonics coefficients); according to the diagonal part only of the covariance matrix of EIGEN-1S, it reduces to 15.5%.

Table 4: Mismodelled classical nodal precessions $\delta\dot{\Omega}_{(2n)}$ and predicted Lense-Thirring nodal precessions $\dot{\Omega}_{\text{LT}}$ of the existing geodetic laser-ranged satellites and of LARES. L1=LAGEOS, L2=LAGEOS II, LR=LARES, Aj=Ajisai, Stl=Stella, Str=Starlette, WS=WESTPAC1, E1=ETALON1, E2=ETALON2. The errors δJ_{2n} are those of the preliminary EIGEN-1S Earth gravity model from 88 days of CHAMP data. All the values are in mas/y. For the ETALON satellites, since all the values are less than 10^{-1} mas/y a – has been inserted.

$2n$	L1	L2	LR	Aj	Stl	Str	WS	E1	E2
2	-3.9	7.2	3.9	35	-11.1	45.1	-10.2	–	–
4	-7.2	2.6	7.3	7.7	-77.7	8.9	-71.7	–	–
6	-3.8	-5.8	3.8	-181.5	-204.5	-313.4	-190.1	–	–
8	-0.4	-2.3	0.4	-83.8	-340.3	-154.3	-320.3	–	–
10	0.4	0.6	-0.4	168.5	-379.6	395.6	-364.6	—	–
12	0.3	0.4	-0.3	125.9	-417	318.2	-413.5	–	–
14	0.1	-0.001	-0.1	-122.1	-441.9	-400.8	-461.3	–	–
16	0.02	-0.07	-0.03	-152	-354.1	-525.6	-404.7	–	–
18	-0.003	-0.01	0.003	49.2	-214	242.2	-299.4	–	–
20	-0.005	0.007	0.006	131.3	-42.2	624.3	-163.9	–	–
$\dot{\Omega}_{\text{LT}}$	30.7	31.6	30.8	116.7	152.8	144.4	151.5	3.4	3.4

5 Conclusions

The systematic error induced by the mismodelled static part of the geopotential is the major source of uncertainty in many tests of General Relativity to be performed in the gravitational field of the Earth via Satellite Laser Ranging. In this paper we have explicitly calculated the expressions of the coefficients of the classical secular precessions of the node and the perigee generated by the even zonal harmonics of the geopotential up to degree $l = 20$. Subsequently, we

Table 5: Mismodelled classical perigee precessions $\delta\dot{\omega}_{(2n)}$ and predicted Lense-Thirring and gravitoelectric perigee precessions $\dot{\omega}_{\text{LT}}$ and $\dot{\omega}_{\text{GE}}$ of the existing spherical passive geodetic laser-ranged satellites and of LARES. L1=LAGEOS, L2=LAGEOS II, LR=LARES, Aj=Ajisai, Stl=Stella, Str=Starlette, WS=WESTPAC1, E1=ETALON1, E2=ETALON2. All the values are in mas/y. The errors δJ_{2n} are those of the preliminary EIGEN-1S Earth gravity model from 88 days of CHAMP data.

$2n$	L1	L2	LR	Aj	Stl	Str	WS	E1	E2
2	—	-4.9	2.4	—	—	-37.8	—	—	—
4	—	-18.3	-2.6	—	—	-288.2	—	—	—
6	—	-4	-11	—	—	96.2	—	—	—
8	—	9.8	-9.7	—	—	1,454.6	—	—	—
10	—	4	-3.6	—	—	574	—	—	—
12	—	-1	-0.6	—	—	-2,112.2	—	—	—
14	—	-1.4	0.4	—	—	-2,425.3	—	—	—
16	—	-0.07	0.3	—	—	2,468.3	—	—	—
18	—	0.2	0.1	—	—	3,794.6	—	—	—
20	—	0.05	0.04	—	—	-1,614.6	—	—	—
$\dot{\omega}_{\text{LT}}$	—	-57.5	-31.6	—	—	68.5	—	—	—
$\dot{\omega}_{\text{GE}}$	—	3,348	3,278.6	—	—	11,804.7	—	—	—

have compared the mismodelled precessions, according to EGM96 gravity model and EIGEN-1S preliminary gravity model which includes 88 days of data from CHAMP, to the general relativistic gravitomagnetic and gravitoelectric secular trends affecting the same orbital elements. While for the LAGEOS family a calculation up to $l = 20$ is well adequate, for the other satellites orbiting at lower altitudes also the other harmonics of higher degrees should be considered. The future, more accurate terrestrial global gravity models from CHAMP and GRACE missions will have a notable impact on the improvement of, among other things, the precision of such general relativistic tests.

References

- [Ciufolini, 1986] Ciufolini, I., Measurement of Lense-Thirring drag on high-altitude laser ranged artificial satellite, *Phys. Rev. Lett.*, 56, 278-281, 1986.
- [Ciufolini and Wheeler, 1995] Ciufolini, I., and J. A. Wheeler, *Gravitation and Inertia*, 498 pp., Princeton University Press, New York, 1995.

- [Ciufolini, 1996] Ciufolini, I., On a new method to measure the gravitomagnetic field using two orbiting satellites, *Il Nuovo Cimento*, 109A, 12, 1709-1720, 1996.
- [Ciufolini et al., 1998] Ciufolini, I., E. Pavlis, F. Chieppa, E. Fernandes-Vieira, and J. Pérez-Mercader, Test of General Relativity and Measurement of the Lense-Thirring Effect with Two Earth Satellites, *Science*, 279, 2100-2103, 1998.
- [Everitt et al., 2001] Everitt, C. W. F., and other members of the Gravity Probe B team, Gravity Probe B: Countdown to Launch, in: Lämmerzahl, C., C.W.F. Everitt, and F.W. Hehl (Eds.), *Gyros, Clocks, Interferometers...: Testing Relativistic Gravity in Space*, Lecture Note in Physics 562, 507 pp., Springer Verlag, Berlin, 2001.
- [Iorio, 2001] Iorio, L., Earth tides and Lense-Thirring effect, *Celest. Mech.*, 79(3), 201-230, 2001b.
- [Iorio and Pavlis, 2001] Iorio, L. and E.C. Pavlis, Tidal Satellite Perturbations and the Lense-Thirring Effect, *J. of the Geod. Soc. of Japan*, 47(1), 169-173, 2001.
- [Iorio et al., 2002a] Iorio, L., I. Ciufolini and E.C. Pavlis, On the possibility of measuring accurately the PPN parameters β and γ with laser-ranged satellites, submitted to *Class. and Quantum Grav.*, gr-qc/0103088, 2001.
- [Iorio et al., 2002b] Iorio, L., I. Ciufolini and D. Lucchesi, paper in preparation, 2002b.
- [Iorio et al., 2002c] Iorio, L., H.I.M. Lichtenegger, and B. Mashhoon, An alternative derivation of the gravitomagnetic clock effect, *Class. and Quantum Grav.*, 19, 39-49, 2002c.
- [Iorio, 2002] Iorio, L., Testing General Relativity with LAGEOS, LAGEOS II and Ajisai laser-ranged satellites, to appear in *J. of the Geodetic Soc. of Japan*, preprint gr-qc/0105014, 2002.
- [Kaula, 1966] Kaula, W. M., *Theory of Satellite Geodesy*, 124 pp., Blaisdell Publishing Company, Waltham, 1966

- [*Lemoine et al.*, 1998] Lemoine, F. G., et al., The Development of the Joint NASA GSFC and the National Imagery Mapping Agency (NIMA) Geopotential Model EGM96, NASA/TP-1998-206861, 1998.
- [*Lense and Thirring*, 1918] Lense, J., and H. Thirring, Über den Einfluss der Eigenrotation der Zentralkörper auf die Bewegung der Planeten und Monde nach der Einsteinschen Gravitationstheorie, *Phys. Z.*, 19, 156-163, 1918, translated by Mashhoon, B., F. W. Hehl, and D. S. Theiss, On the Gravitational Effects of Rotating Masses: The Thirring-Lense Papers, *Gen. Rel. Grav.*, 16, 711-750, 1984.
- [*Lucchesi*, 2001] Lucchesi, D., Reassessment of the error modelling of non-gravitational perturbations on LAGEOS II and their impact in the Lense-Thirring determination. Part I, *Plan. and Space Sci.*, 49, 447-463, 2001.
- [*Mashhoon et al.*, 1999] Mashhoon, B., F. Gronwald, and D.S. Theiss, On Measuring Gravitomagnetism via Spaceborne Clocks: A Gravitomagnetic Clock Effect, *Annalen Phys.*, 8, 135-152, 1999.
- [*Pavlis and Iorio*, 2002] Pavlis, E. C., and L. Iorio, The impact of tidal errors on the determination of the Lense-Thirring effect from satellite laser ranging, to be published in *Int. J. of Mod. Phys. D*, gr-qc/0007015, 2002.